Measured wind turbine loads and their dependence on inflow parameters

L. Manuel & L. D. Nelson
Dept. of Civil Engineering, University of Texas at Austin, TX, USA

H. J. Sutherland & P. S. Veers
Sandia National Laboratories, Wind Energy Technology Department, Albuquerque, NM 87185, USA

Keywords: fatigue loads, extreme loads, wind turbines, inflow, turbulence

ABSTRACT: The Long-Term Inflow and Structural Test (LIST) program is gathering inflow and structural response data on a Westinghouse 600-kW wind turbine located at a test site near Boulder, Colorado. Data from 1043 ten-minute time segments are analyzed here to determine the dependency of fatigue and extreme loads on inflow parameters. Flap and edge bending moment ranges at the blade root are studied as the structural response variable of interest. Various parameters related to the inflow (including primary parameters such as the mean and standard deviation of the hub-height horizontal wind speed as well as secondary parameters such as Reynolds stresses, vertical shear exponent, etc.) are each considered in an inflow parameter vector. Time series for the structural response are processed in order to obtain a structural response parameter, which in separate statistical studies, is taken to be either an equivalent fatigue load or an extreme load. We describe a procedure by which the important "dependencies" of response on the various variables contained in the inflow parameter vector may be determined considering all the available data. The procedure employed is similar to other previous studies, but we do not bin the data sets by wind speed since dependencies in one wind speed bin may be different from those in other bins. Also, our procedure, in sharp contrast to previous studies, examines each inflow parameter in the vector in a sequential analysis, rather than by using multivariate regression.

1 INTRODUCTION

Of fundamental importance to any study of site-specific design loads for wind turbines is the understanding of the extent to which inflow (wind) parameters influence turbine loads. Inflow parameters might include, for example, mean wind speed, turbulence intensity, roughness length, transverse turbulence, and turbulence length scales for each wind component.

One of the sites instrumented as part of the Long-Term Inflow and Structural Test (LIST) program is at the National Renewable Energy Laboratory's National Wind Technology Center (NWTC) near Boulder, Colorado. This program has made available detailed atmospheric inflow conditions and structural response data from a wind turbine over a significantly long period (October 2000 to May 2001). In a previous study, Sutherland and Kelley (2003) employed the LIST data to assess the influence of atmospheric conditions on damage-equivalent fatigue loads. This same data set is employed in the present study which seeks to determine the dependencies that exist in blade root flap and edge bending moment fatigue and extreme loads on various inflow parameters.

In contrast with previous analysis of these data, we seek here to examine the ability of inflow parameters to explain the response behavior of a turbine sequentially (i.e., considering one inflow parameter at a time), rather than with a multivariate approach. Since there is a well-accepted practice of using the mean and standard deviation of the horizontal wind speed at the hub height to characterize the design environment, the dependence of response on these two inflow parameters is first extracted from the loads data. Then, the next most influential input parameter is identified and extracted. The goal is that such a procedure can provide a measure of

which parameters are most likely to add understanding of the site influence on turbine loads in addition to ones already in use. Also, the need, as in a multivariate regression, for the inflow parameters (independent variables) to be statistically independent is removed.

2 THE FIELD MEASUREMENT CAMPAIGN

The Advanced Research Turbine (ART) used in this measurement campaign is a Westinghouse 600-kW turbine (Snow et al., 1989) currently located at a site near Boulder, Colorado. A short description of the turbine and the measurement campaign is included.

2.1 *The Turbine*

The Westinghouse 600-kW turbine, see Fig. 1, is an upwind, two-bladed teetered-hub machine. It has full span pitch control and a synchronous generator. The turbine has a rotor diameter of 42 m and a hub height of 36.6 m. It is a constant speed (43 rpm) machine that reaches rated wind power at 12.8 m/s. Its cut-in and cut-out wind speeds are 6.25 m/s and 22.3 m/s, respectively. The turbine is fitted with blades made from a wood/epoxy laminate – the first bending frequency of the blade when mounted to the hub is 2.24 Hz in the flapwise (out-of-plane) direction and 4.56 Hz in the edgewise (in-plane) direction.

Figure 1. The Turbine and the 42-m Inflow Measurement Array Upwind of the Turbine.

2.2 *The Data*

A 42-m diameter planar array consisting of five high-resolution ultrasonic anemometers and supporting meteorological instrumentation was installed 1.5 diameters in a direction predominantly upwind of the turbine. From the wind turbine, a number of aeroelastic, structural, and supporting measurements were also collected. The data were recorded and stored as ten-minute segments. A total of 3299 ten-minute records are available in this data set. This analysis uses a subset of the data (comprising 1043 ten-minute records) for which mean wind speeds were greater than 9 m/s and the mean wind direction was within ±45 degrees off the perpendicular to the planar array. Figure 2 shows a distribution of the records used, classified according to mean horizontal wind speed.

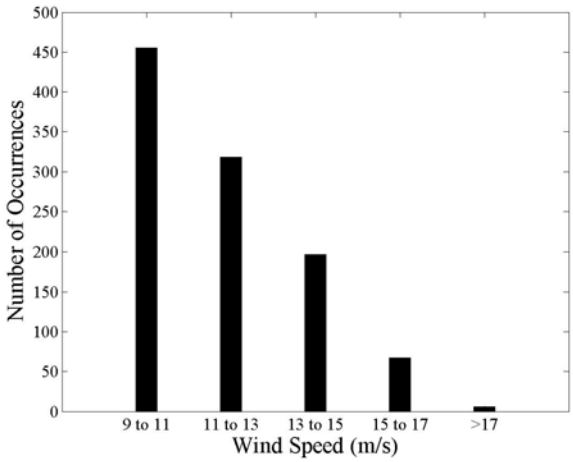

Figure 2. Distribution of 10-Minute Records Classified by Mean Wind Speed.

3 NUMERICAL STUDIES

Several authors have examined the influence of inflow parameters on fatigue loads. Fragoulis (1997), Glinou and Fragoulis (1996), and Sutherland (2001) have examined the influence of various inflow parameters on equivalent fatigue loads. Kelley (1994) has examined the influence of several parameters on the shape of the fatigue spectrum. The present work is one more study aimed at determining the influence of inflow parameters on both equivalent fatigue loads as well as extreme loads. Data from the LIST program are employed in this study.

3.1 *Structural Response*

In the following, the structural response defined by the variable, z, taken directly from the available ten-

minute time series records will represent the edge or the flap bending moment at the root of a blade. The time series representing z are processed to yield the variable, y, which is chosen to be, in separate statistical analyses, first, the damage-equivalent fatigue loads derived from blade root bending moments, and next, the maximum or extreme bending moment. The damage-equivalent load is the constant-amplitude load of a specified number of cycles (here, taken to be 1000) in 10 minutes that produces equivalent damage to the actual amount of damage resulting from the measured variable-amplitude load cycles (Sutherland, 1999). The extreme load is the largest load amplitude in each 10-minute sample. The purpose of the proposed analysis is to determine the influence of the inflow parameters on damage-equivalent fatigue loads as well as extreme loads.

3.2 *Inflow Parameters*

The atmospheric time series data are processed to form an inflow parameter vector, $\boldsymbol{x}$, which is used as the independent variable. This vector consists of a primary inflow parameter vector, $\boldsymbol{x}_p$, and a secondary inflow parameter vector, $\boldsymbol{x}_s$. The wind turbine community has a widely held practice of using the horizontal mean wind speed at hub height and a measure of turbulence, such as the standard deviation of horizontal wind speed, as the primary factors that influence fatigue and extreme loads. Accordingly, $\boldsymbol{x}_\mathrm{p}$, the primary inflow parameter vector, is defined to consist of the mean (μ) and standard deviation (σ) of horizontal wind speed.

The vector $\boldsymbol{x}_\mathrm{s}$ is defined to consist of thirteen secondary inflow wind parameters. Included in this vector are: the vertical wind shear exponent over the rotor (α), the standard deviations of wind speed in the cross-wind and vertical directions (σ_v and σ_w), the mean turbulence kinetic energy (KE), the three orthogonal mean Reynolds stresses ($u'w'$, $u'v'$, and $v'w'$), the local friction velocity (U^*), the gradient Richardson number (Ri), and the skewness (S_u) and kurtosis (K_u) of horizontal wind speed. Various authors have proposed one or more of these parameters previously. Rohatgi and Nelson (1994) summarize descriptions of many of these parameters. Fragoulis (1997), Glinou and Fragoulis (1996), Kelley and McKenna (1996), and Kelley et al (1997) also propose these and other parameters in studying wind turbine loads. Sutherland (2001) provides a mathematical description for each of these $\boldsymbol{x}_\mathrm{s}$ variables.

Equation (1) below summarizes the various primary and secondary inflow parameters used in this study:

$$\begin{aligned} &\boldsymbol{x} = \{\boldsymbol{x}_p, \boldsymbol{x}_s\}; \quad \boldsymbol{x}_p = \{\mu, \sigma\}; \\ &\boldsymbol{x}_s = \{\alpha, \sigma_v, \sigma_w, KE, u'w', u'v', v'w', U^*, Ri, S_u, K_u\} \end{aligned} \tag{1}$$

3.3 *Regression*

We describe the initial regression that was performed of the response, y, on the primary inflow parameter vector, $\boldsymbol{x}_\mathrm{p}$.

$$\begin{aligned} &\hat{y} = \boldsymbol{A}_0 \boldsymbol{L}(\boldsymbol{x}_p)^T + B_0; \quad y - \hat{y} = \varepsilon_1 \\ &\boldsymbol{A}_0 = [A_{01}\ A_{02}\ A_{03}\ A_{04}]; \quad \boldsymbol{L}(\boldsymbol{x}_p) = [\mu\ \sigma\ \mu^2\ \sigma^2] \end{aligned} \tag{2}$$

where $\boldsymbol{A}_0$ and B_0 are estimated by regression techniques using terms up to second order involving the two primary inflow parameters, μ and σ. Other models for this initial regression on primary inflow parameters have been suggested such as power law and logarithmic forms for both fatigue and extreme loads (see Veers and Winterstein (1998), Manuel et al (2001), and Moriarty et al (2002)). These forms were also attempted here but were found to yield smaller coefficients of determination relative to the form of the regression equation shown in Eq. (2). As such, the quadratic model was adopted.

After this initial regression was performed, the residual, ε_1 (the difference between the *observed* value, y, of the dependent variable, and the *predicted* value, $\hat{y}$, resulting from a least squares regression using Eq. (2)) was next regressed on a *single* parameter from the secondary inflow parameter vector, $\boldsymbol{x}_\mathrm{s}$, as shown in Eq. (3). The selection of one particular element of $\boldsymbol{x}_\mathrm{s}$ was made based on the correlation coefficient between ε_1 and each element of $\boldsymbol{x}_\mathrm{s}$. The element in $\boldsymbol{x}_\mathrm{s}$ that has the highest correlation with ε_1 is chosen as $x_{s,1}$.

$$\varepsilon_1 = A_1 x_{s,1} + B_1 + \varepsilon_2; \quad \ldots \quad \varepsilon_i = A_i x_{s,i} + B_i + \varepsilon_{i+1} \tag{3}$$

$$\theta_i = 1 - SE_i / SE_{i-1}; \qquad SE_i = \sum_{j=1}^{N} (\varepsilon_i^2)_j \text{ for } i \geq 2 \tag{4}$$

where $(\varepsilon^2{}_i)_j$ represents the squared residual from data set j of the N sets (note that N is equal to 1043, the total number of data sets used) after the ith regression. Only linear models were considered for regression of the residuals on the secondary inflow parameters.

Equation (3) shows how the residual, ε_i, from any step i during this procedure of regression on one element of $\boldsymbol{x}_\mathrm{s}$ (indicated here by $x_{s,i}$) leads to a new residual, ε_{i+1} and the regression procedure continues. The degree of influence that any variable, $x_{s,i}$, has on the response variable, y, is assessed by the parameter, θ_i, in Eq. (4) since θ_i quantifies the reduction in the sum of the squared residuals in step i (relative to step i-1). Thus, a small value of θ_i is an indication

that there is no significant benefit of the regression on $x_{s,i}$ in influencing or helping explain the response variable, y. Alternatively, a large value of θ_i, indicates that $x_{s,i}$ does help in predicting or explaining y better. After the initial regression on $x_{s,1}$, the order of selection of each subsequent element of $\boldsymbol{x}_s$ corresponds to the parameter with the highest correlation coefficient between ε_i and each of the unaccounted-for elements of $\boldsymbol{x}_s$. Thus, after each regression step dealing with the parameter, $x_{s,i}$ in the secondary inflow vector, $\boldsymbol{x}_s$, a newly computed correlation matrix of ε_{i+1} with the remaining parameters of $\boldsymbol{x}_s$ guides the next choice, $x_{s,i+1}$ and the procedure continues; it is stopped when the value of θ_i approaches zero.

This analysis is in sharp contrast to the analyses performed by Fragoulis (1997), Glinou and Fragoulis (1996), and Sutherland (2001). In particular, a sequential analysis is presented here, while the referenced studies use a single multivariate regression to determine the influence of all the inflow parameters simultaneously. Also, those earlier studies considered dependency of response on secondary inflow parameters separately for different inflow conditions described by wind speed ranges (or bins). The current procedure seeks to explain how primary and inflow parameters together influence wind turbine loads over *all* inflow conditions (i.e., not for separate bins). This procedure takes into consideration correlation among the secondary inflow parameters while the referenced studies do not.

4 DATA ANALYSIS

4.1 *Dependent Variable – Fatigue Loads*

The blade root fatigue loads for the flap- and edge-wise bending moment are each considered separately as the dependent variable, y. These are characterized using damage-equivalent fatigue loads (see Sutherland, 1999) and are determined for two fatigue exponents, m, equal to 3 and 10. The former yields an equivalent fatigue load appropriate for welded steel and the latter for fiberglass composites.

Regression analyses were carried out where y given by Eq. (2) represented four different variables corresponding to damage-equivalent root edge or flap bending moments for m equal to 3 or 10.

4.2 *Dependent Variable – Extreme Loads*

The extreme blade root flap- and edge-wise bending moments are next considered as the dependent variable, y. The maximum or extreme load is another measure of the severity of a load spectrum of interest for the design of wind turbines. For this analysis, the single largest maximum flap- and edge-wise bending moment value determined from each ten-minute time series was employed.

Regression analyses were carried out where y given by Eq. (2) represented two different variables corresponding to extreme root edge or flap bending moments.

4.3 *Numerical Studies*

The regression procedure outlined above and described by Eqs. (1-4) was employed for the analysis of several different response time series.

The available data set of 1043 ten-minute data segments was used to study the dependencies of flap and edge bending moment fatigue (damage-equivalent) loads for m equal to 3 and 10 on the various inflow parameters in $\boldsymbol{x}_p$ and $\boldsymbol{x}_s$. The dependency of flap and edge extreme loads on the inflow parameters was also examined for this data set.

It should be noted that the selection of mean wind speed and standard deviation of wind speed as "primary" inflow parameters was confirmed as being the most appropriate since we found that the correlation coefficient for each of these two parameters with any choice for variable, y, was larger than that for any of the secondary inflow parameters in the vector, $\boldsymbol{x}_s$.

5 RESULTS

The data set upon which the results are based consists of 1043 ten-minute records of inflow and structural response measurements. Each of these records had a mean wind speed greater than 9 m/s.

5.1 *Fatigue Loads*

Figures 3a-3d show results from the bivariate regression of the equivalent fatigue load portion of y performed on the primary inflow parameter vector, $\boldsymbol{x}_p$. Figures 3a and 3b are for the fatigue damage-equivalent edge bending moments for m equal to 3 and 10, respectively. Similarly, Figs. 3c and 3d are for the damage-equivalent flap bending moments for m equal to 3 and 10, respectively. The regression surface is not shown; instead, the data are shown along with a plot of y versus the mean horizontal wind speed. To represent a range of typical values for the other primary inflow parameter, namely the standard deviation of the horizontal wind speed, σ (denoted as sigma in the figures), three curves based on the regression results and representing σ values of 1.0, 2.0, and 3.0 m/s are also shown. The distance between the curves is an indication of the influence of σ on the loads in each case.

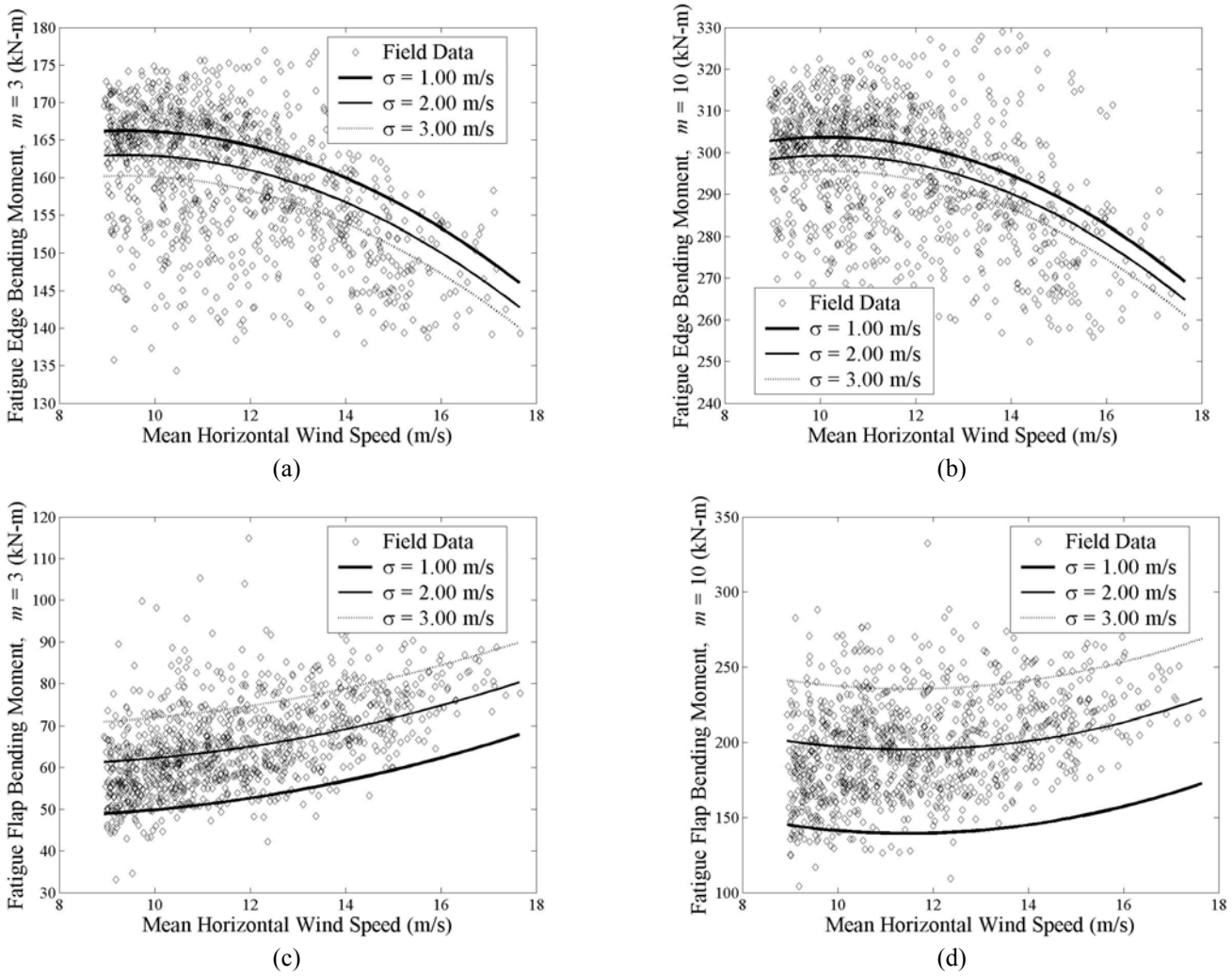

Figure 3. Damage-equivalent fatigue bending moments versus wind speed.

Figure 4 shows correlation coefficients for the residual, ε_1 (see Eq. (3)) with elements of the secondary inflow vector, $\boldsymbol{x}_s$, after regression of y (in this case, damage-equivalent fatigue loads in the edge and flap bending modes for m equal to 3 and 10) on $\boldsymbol{x}_p$. The low correlation coefficients indicate that performing further regressions on $\boldsymbol{x}_s$ will not significantly reduce the residuals compared to what was already achieved after regression of y on $\boldsymbol{x}_p$. To illustrate this, Table 1 shows the results of five additional regressions of residuals, ε_i, performed on one parameter of $\boldsymbol{x}_s$ at a time. Results are shown for all four cases described above (namely, fatigue damage-equivalent edge and flap bending moments with fatigue exponent, m equal to 3 and 10).

As defined earlier, the θ_i term in general describes how much of the variance in residuals is explained by the regression. Note that θ_0 is equivalent to the coefficient of determination, R^2, after the first regression. As an illustration, $\boldsymbol{x}_p$ explains anywhere from 18 to 64 percent of the variance of the residuals, or, equivalently, the regression of y on $\boldsymbol{x}_p$ never leads to R^2 values greater than 0.64. The implication is that y cannot be adequately predicted by the primary inflow parameters, $\boldsymbol{x}_p$, alone – a fact that can be confirmed by the data shown in Figs. 3a-3d.

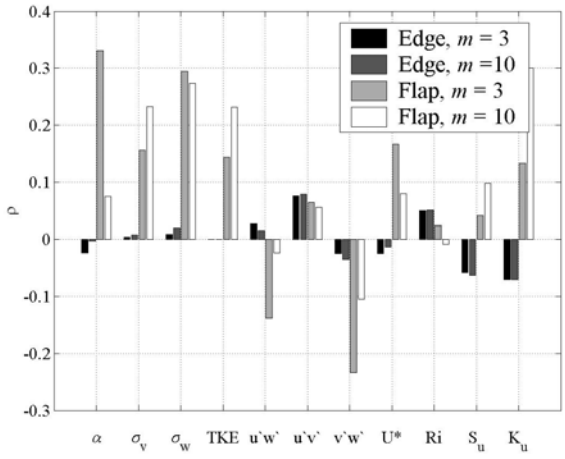

Figure 4. Correlation coefficients between residual after primary regression, ε_1, and $\boldsymbol{x}_s$ for damage-equivalent fatigue loads.

i	x	$\boldsymbol{A}_i$	B_i	θ_i
0	$\boldsymbol{x}_p$	[5.60, -3.99, -0.30, 0.25]	143.64	0.2496
1	$u'v'$	0.52	-0.25	0.0058
2	K_u	-1.08	-0.20	0.0047
3	Ri	8.86	-0.13	0.0029
4	$u'w'$	1.05	0.44	0.0018
5	σ_w	1.29	-1.31	0.0015

(a) Edge, m=3.

i	x	$\boldsymbol{A}_i$	B_i	θ_i
0	$\boldsymbol{x}_p$	[12.47, -5.49, -0.61, 0.36]	245.50	0.1827
1	$u'v'$	1.01	-0.48	0.0062
2	K_u	-2.02	-0.38	0.0047
3	Ri	17.15	-0.25	0.0031
4	$v'w'$	-1.71	-0.29	0.0014
5	S_u	-1.82	0.26	0.0015

(b) Edge, m=10.

i	x	$\boldsymbol{A}_i$	B_i	θ_i
0	$\boldsymbol{x}_p$	[-2.39, 16.53, 0.17, -1.38]	41.46	0.5541
1	α	70.37	-9.02	0.1095
2	σ_w	10.54	-10.72	0.1266
3	K_u	1.35	0.25	0.0110
4	$u'w'$	1.50	0.63	0.0055
5	$v'w'$	-1.64	-0.28	0.0070

(c) Flap, m=3.

i	x	$\boldsymbol{A}_i$	B_i	θ_i
0	$\boldsymbol{x}_p$	[-20.13, 79.83, 0.88, -7.97]	183.11	0.6364
1	K_u	12.22	2.30	0.0900
2	σ_w	21.28	-21.65	0.0647
3	σ_v	1.34	-4.19	0.0121
4	α	57.48	-7.36	0.0111
5	$u'w'$	6.17	2.59	0.0109

(d) Flap, m=10.

Table 1: Regression Results for Damage-Equivalent Fatigue Loads.

The parameters from $\boldsymbol{x}_s$ shown for i equal to 1-5 in Table 1 are selected based on the highest correlation coefficient of that parameter with the residual from the preceding regression. Thus, for example, for the damage-equivalent edge bending moment with m equal to 3, the parameters of $\boldsymbol{x}_s$ selected are in sequence, the orthogonal u-v mean turbulent Reynolds stress component ($u'v'$), the kurtosis of the horizontal wind speed (K_u), the gradient Richardson number (Ri), the orthogonal u-w mean turbulent Reynolds stress component ($u'w'$), and the standard deviation of the wind speed in the vertical wind speed (σ_w). It is clear that none of the parameters in $\boldsymbol{x}_s$ has significant influence on reducing the residuals in y in the case of fatigue damage-equivalent bending moments in edge or flap modes. This can be seen by the low values of θ_i for all i>0. This also suggests that no secondary inflow parameter usefully contributes to explanation of edge and flap bending fatigue loads once the primary variables of mean wind speed and standard deviation of wind speed are accounted for.

5.2 *Extreme Loads*

Figures 5a and 5b show results from the bivariate regression of the extreme loads, y, on the primary inflow parameter vector, $\boldsymbol{x}_p$. Figure 5a is for the extreme edge bending moment while Fig. 5b is for the extreme flap bending moment. Again, the regression surface is not shown; instead, the data are shown along with a plot of y versus the mean horizontal wind speed for three values of the standard deviation (σ) of the horizontal wind speed (1.0, 2.0, and 3.0 m/s). For extreme loads, there is clearly a quadratic variation with wind speed. Also, the influence of σ is larger for edgewise loads than for flapwise loads.

Figure 6 shows correlation coefficients for the residual, ε_1, with elements of the secondary inflow vector, $\boldsymbol{x}_s$, after regression of y on $\boldsymbol{x}_p$. The correlation coefficients are still fairly low as was the case for the fatigue loads described earlier. Further regressions on $\boldsymbol{x}_s$ do not significantly reduce the residuals compared to their values after regression of y on $\boldsymbol{x}_p$ as can be seen in Table 2.

In the case of the extreme loads, $\boldsymbol{x}_p$ explains no greater than 55 percent of the variance of the residuals (or, equivalently, the regression of y on $\boldsymbol{x}_p$ leads to R^2 values of only 0.55 at best – not much better regression fits of y to $\boldsymbol{x}_p$ than was the case with fatigue loads). Table 2 also shows the sums of squared residuals and the regression coefficients through each step of the procedure. Again, as an example, for the extreme flap loads, the parameters of $\boldsymbol{x}_s$ selected are in sequence, K_u, σ_w, S_u, α, and KE, but again it is clear that none of the parameters in $\boldsymbol{x}_s$ has significant influence on reducing the residuals in y in the case of extreme bending moments in edge or flap mode. This can be seen by the low values of θ_i

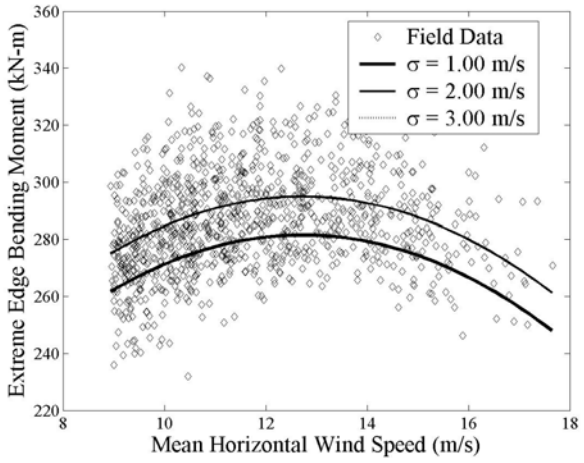

(a)

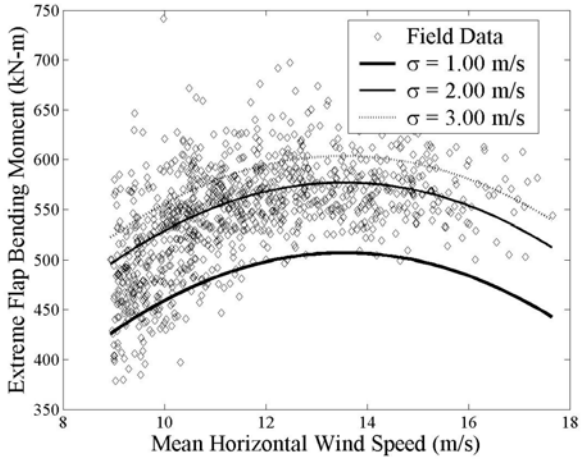

(b)

Figure 5. Extreme edge and flap bending moment versus wind speed.

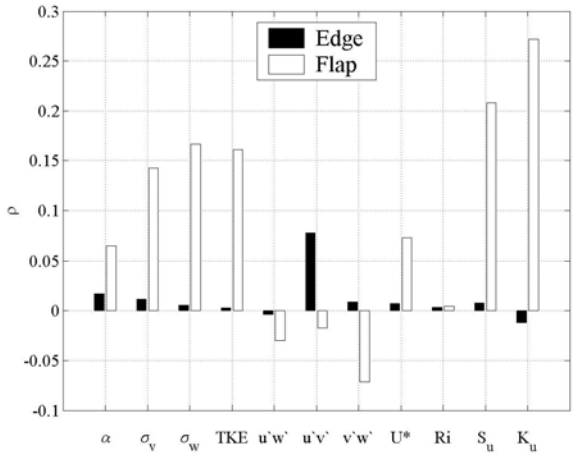

Figure 6. Correlation coefficients between residual after primary regression, ε_1, and $\boldsymbol{x}_s$ for extreme loads.

for all $i>0$. This also suggests that no secondary inflow parameter usefully contributes to prediction of edge and flap bending extreme loads.

i	x	$\boldsymbol{A}_i$	B_i	θ_i
0	$\boldsymbol{x}_p$	[35.28, 33.39, -1.39, -6.69]	30.39	0.1773
1	$u'v'$	1.14	-0.54	0.0061
2	$v'w'$	0.99	0.17	0.0004
3	σ_v	0.24	-0.74	0.0005
4	α	8.59	-1.10	0.0003
5	$u'w'$	0.82	0.34	0.0002

(a) Edge.

i	x	$\boldsymbol{A}_i$	B_i	θ_i
0	$\boldsymbol{x}_p$	[103.80, 134.50, -3.83, -21.55]	-308.70	0.5534
1	K_u	19.90	3.75	0.0740
2	σ_w	21.89	-22.28	0.0209
3	S_u	8.96	-1.28	0.0066
4	α	83.81	-10.74	0.0068
5	KE	0.25	-2.43	0.0036

(b) Flap.

Table 2: Regression Results for Extreme Loads.

6 CORRELATION OF INFLOW PARAMETERS

The degree of correlation among the various inflow parameters makes it difficult to unambiguously identify the parameters that influence turbine loads. When one parameter is strongly correlated with another, even though each might be influential to some extent, the first might serve as a surrogate for the second.

The data set suggests that there exists strong correlation between, on the one hand, any one of the two primary inflow parameters, and, on the other hand, one or more of the secondary inflow parameters. Only a few of these secondary parameters were relatively uncorrelated with the primary parameters. Therefore, each of the remaining parameters has their relationship with or influence on the response variables largely accounted for by the relationship between the response and the primary parameters. The fact that one parameter can act as a surrogate for another leaves open the possibility that some secondary parameter may in fact be important in driving the magnitude of turbine response.

7 DISCUSSION AND CONCLUSIONS

Data available on inflow and structural response from the LIST program have provided an opportu-

nity to study the influence of various inflow parameters on fatigue and extreme wind turbine loads. A procedure is presented that employed several steps involving regression of loads on primary and secondary inflow parameters. Residuals obtained in each regression step helped in identifying which inflow parameter might be a candidate for regression after more important parameters had already been considered. A systematic approach was followed for damage-equivalent fatigue loads with fatigue exponents of 3 and 10, and for extreme loads representing root flap and edge bending moments.

In general, it was found that the fatigue and extreme loads showed few dependencies on either the primary or the secondary inflow parameters.

Results from this study suggest that the large correlation coefficients between several of the secondary parameters individually and each of the primary parameters make it difficult for the secondary parameters to provide any additional explanation of turbine response once the primary parameters have been accounted for.

ACKNOWLEDGEMENTS

The authors gratefully acknowledge the financial support provided by Grant No. 003658-0272-2001 awarded through the Advanced Research Program of the Texas Higher Education Coordinating Board.

REFERENCES

Fragoulis, A.N., 1997. The Complex Terrain Wind Environment and its Effects on the Power Output and Loading of Wind Turbines, *Proc. 1997 ASME Wind Energy Symp.*, pp. 33-40.

Glinou, G. and A. Fragoulis, eds., 1996. Mounturb Final Report, 3 volumes, *JOU2-CT93-0378*.

Kelley, N.D., 1994. The Identification of Inflow Fluid Dynamics Parameters that can be used to scale Fatigue Loading Spectra of Wind Turbine Structural Components, *Proc. 1994 ASME Wind Energy Symp.*, ASME, pp. 181-196.

Kelley, N. D. and McKenna, H. E., 1996. The Evaluation of a Turbulent Loads Characterization System, *Proc. 1996 ASME Wind Energy Symp.*, ASME, pp. 69-77.

Kelley, N. D., Hand, M., Larwood, S. and McKenna, E., 2002. The NREL Large-Scale Turbine Inflow and Response Experiment – Preliminary Results, *Proc. 2002 ASME Wind Energy Symp.*, AIAA/ASME, pp. 412-426.

Kelley, N. D., Wright, A. D., Buhl, Jr., M. L. and Tangler, J. L., 1997. Long-Term Simulation of Turbulence-Induced Loads Using the SNL WIND-3D, FAST, YawDyn, and ADAMS Numerical Codes, *Proc. 1997 ASME Wind Energy Symp.*, ASME, pp. 74-85.

Manuel, L., Veers, P. S. and Winterstein, S. R., 2001. Parametric Models for Estimating Wind Turbine Fatigue Loads for Design, *Journal of Solar Energy Engineering, Trans. of the ASME*, Vol. 123, No. 4, pp. 346-355.

Moriarty, P. J., Holley, W. E. and Butterfield, S., 2002. Effect of Turbulence Variation on Extreme Loads Prediction for Wind Turbines, *Journal of Solar Energy Engineering, Trans. of the ASME*, Vol. 124, No. 4, pp. 387-395.

Rohatgi, J. S. and Nelson, V., 1994. Wind Characteristics – An Analysis for the Generation of Wind Power, *Alternative Energy Institute*, Canyon, TX, 237p.

Snow, A. L., Heberling, II, C.F. and Van Bibber, L. E., 1989. The Dynamic Response of a Westinghouse 600-kW Wind Turbine, *SERI/STR-217-3405*, Solar Research Institute.

Sutherland, H. J., 1999. On the Fatigue Analysis of Wind Turbines, *SAND99-0089*, Sandia National Laboratories, Albuquerque, NM, 132 p.

Sutherland, H. J., 2001. Preliminary Analysis of the Structural and Inflow Data from the LIST Turbine, *Proc. 2001 ASME Wind Energy Symp.*, AIAA-2001-0041, pp. 1-12.

Sutherland, H. J., P. L. Jones and B. Neal, 2001. The Long-Term Inflow and Structural Test Program, *Proc. 2001 ASME Wind Energy Symp.*, AIAA-2001-0039.

Sutherland, H. J. and Kelley, N. D., 2003. Inflow and Fatigue Response of the NWTC Advanced Research Turbine, *Proc. 2003 ASME Wind Energy Symp.*, AIAA-2003-0862, pp. 214-224.

Veers, P. S. and Winterstein, S. R., 1998. Application of Measured Loads to Wind Turbine Fatigue and Reliability Analysis, *Journal of Solar Energy Engineering, Trans. of the ASME*, Vol. 120, No. 4.